Enhancing synergy for power generation and coastal protection through wave energy converters

Beatrice Battisti, Giuseppe Giorgi, Gael Verao Fernandez

Enhancing synergy for power generation and coastal protection through wave energy converters

B. Battisti
Marine Offshore Renewable Energy Lab (MOREnergy Lab), Politecnico di Torino, Italy
Université de Bordeaux, IMB, France

G. Giorgi
Marine Offshore Renewable Energy Lab (MOREnergy Lab), Politecnico di Torino, Italy

G. Verao Fernandez
Department of the Built Environment, Aalborg University, Denmark

ABSTRACT: Combining efforts to promote both power generation and coastal protection would offer significant advantages for the marine sector. It presents an opportunity to combine resources for the dual purpose of adapting to the effects of climate change, and producing clean energy, thereby potentially fostering growth in the blue economy. Wave Energy Converters (WECs), and particularly WEC farms, are ideally suited to fulfill this dual role, as they can harvest energy from waves, thus also mitigating their impact on coastlines, with the generation of milder waves in their lee. This research investigates the impact of a small WEC farm on both objectives. Different strategies are proposed, and compared, to address this dual focus. Strategies may involve establishing a minimum threshold for wave attenuation, while maximizing power production, and others aim to optimize both power production, and wave attenuation simultaneously. The former strategies can be easily tailored to meet specific coastal protection requirements, at a particular site. The latter entail addressing a bi-objective optimization problem, with two concurrent objectives. This paper explores these different approaches, ultimately laying the groundwork for a comprehensive multi-query analysis of WEC farms.

1 INTRODUCTION

In recent years, the significance of offshore renewable energy sources in attaining net zero energy goals and achieving complete decarbonization has become increasingly apparent: these sources serve as valuable complements to the energy mix, offering diversity and resilience (Novo et al. 2022). While offshore wind is expected to play a substantial role in total installed capacity, Wave Energy Converters (WECs) are envisioned to provide a dependable and consistent base load, thereby alleviating the need for extensive energy storage solutions (Kardakaris et al. 2021). However, individual WECs typically possess relatively modest rated power compared to grid demands; in addition, the capital (CapEx) and operational (OpEx) costs associated with WECs are often considerable (Giglio et al. 2023). Consequently, it is frequently advantageous to aggregate WECs into farms (Foteinis & Tsoutsos 2016).

The primary and most intuitive objective of a WEC farm is to maximize overall power capture, while minimizing the Levelized Cost of Energy (LCoE). Cost minimization is closely intertwined with reducing the overall footprint of the farm, since greater distances between WECs necessitate longer cable connections and potentially higher operational expenses. Consequently, it is generally reasonable to assume that minimizing costs also involves minimizing the distance between WECs. However, the interaction between waves and WEC structures introduces intricate modifications to the surrounding wave field, including diffraction and radiation effects. Consequently, identifying the optimal WEC-WEC coupling arrangement is often challenging and non-intuitive. Indeed, depending on the characteristics of both the floaters and the waves, alternating regions of detrimental and potentially beneficial interactions can arise. Furthermore, the influence of WEC-WEC interactions is influenced by the farm layout. In a study by Penalba et al. (2017), the authors evaluate the power production of an array across various inter-device distances in realistic wave climates, discovering that small dis-

tances and large farm sizes exacerbate detrimental interactions, leading to power losses.

A significant portion of the current research in this domain focuses on optimizing power output by modifying the spatial configuration of WEC farms and potentially altering the number of devices (Göteman et al. 2020, Abdulkadir et al. 2023). In this study, a farm comprising five Oscillating Wave Surge Converters (OSWCs) is examined, in both aligned and staggered layouts. To keep the analysis straightforward, the distance between the devices is kept constant. The behavior of this small cluster of OSWCs is considered a useful model for predicting the behavior of larger groups of such clusters, even if some unique dynamics emerge in larger farms. Beyond layout optimization, recent work has tackled the challenge of maximizing energy production in wave energy farms through various control strategies (Ringwood et al. 2023). Centralized, distributed, and decentralized approaches have been explored, each with differing impacts on the overall productivity of these farms. Additionally, progress in the field has led to the release of an open-access dataset derived from a wave tank experimental campaign with up to five WECs (Faedo et al. 2023).

Beyond their primary function of renewable energy production, WEC farms offer secondary benefits, such as coastal protection (Foteinis 2022). Given the escalating concerns over coastal erosion, exacerbated by climate change effects (Kazimierczuk et al. 2023), this aspect has garnered increased attention. Traditional coastal protection measures may bring adverse impacts on marine life, turbidity, and visual aesthetics. WECs, by modifying the wave field in their lee, hold promise for mitigating some of these issues, although localized increases in wave height near the devices may occur. Despite typically being considered a secondary outcome, the coastal protection afforded by WEC farms could prove pivotal in decision-making processes. By incorporating WEC farms into coastal protection strategies, significant reductions in erosion-related costs and risks can be achieved, thus enhancing the economic viability of WECs (Foteinis & Tsoutsos 2016). In literature, several studies have investigated the wave attenuation capabilities of WEC farms, primarily focusing on overtopping or flap-type devices (Tănase Zanopol et al. 2014, Khojasteh et al. 2023).

Given the potentially conflicting goals of optimizing power generation and coastal protection, the common practice is of optimizing for one objective while evaluating the impact on the other post-optimization. Conversely, Battisti et al. (2024) propose to perform a multi-query analysis, where the optimisation objective encompasses, to some extent, both power generation and coastal protection. Indeed, Battisti et al. (2024) demonstrate that the interplay between such objectives is not straightforward and it is necessary to embed some user-driven constraints to enable a definitive solution to the multi-dimensional problem.

Consequently, the novelty of the present paper is to suggest and contrast various approaches to tackle this dual objective. Some strategies propose setting a minimum threshold for wave attenuation while maximizing power output, while others strive to optimize both power generation and wave attenuation simultaneously. The former strategies can be customized to fulfill specific coastal protection needs at particular locations, while the latter involve addressing a bi-objective optimization challenge with two simultaneous goals. This study delves into these diverse methodologies, ultimately paving the way for a thorough multi-query examination of WEC farms.

The reminder of the paper is organized as follows: Sect. 2 presents the numerical model, which is applied to the specific case study described in Sect. 3. Results are then presented in Sect. 4, while Sect. 5 draws some final conclusions and considerations.

2 NUMERICAL MODEL

The BEM (Boundary Element Method), the numerical model used in this study, is based on the potential flow theory, where the fluid is assumed to be inviscid and incompressible, and the flow irrotational. This allows to define a velocity potential $\Phi(\mathbf{x}, t) = \mathrm{Re}[\phi(\mathbf{x})\,\mathrm{e}^{\mathrm{i}\omega t}]$, with the spatial variable $\mathbf{x} = (x, y, z)$, and the temporal variable t, that satisfies the Laplace's equation $\nabla^2\phi = 0$ in the entire domain, with ω the angular wave frequency.

With the assumption of linearity, that holds for small amplitude motions of a body in the domain, and small wave amplitude, the superposition of the potential is applied as:

$$\phi^P = \phi^I + \phi^D + \mathrm{i}\omega \sum_{\delta=1}^{N_{DOF}} \zeta_\delta \phi_\delta^R, \tag{1}$$

where the perturbed potential of a unit amplitude wave, ϕ^P, is given by the superposition of the the incident ϕ^I, radiated ϕ^R, and diffracted ϕ^D potentials. The radiated potential is further related to the body's motions - the N_{DOF} Degrees of Freedom (DoFs) - through the Response Amplitude Operator (RAO) of the δ-th degree of freedom. Defining the gravity g, the free surface can be calculated as:

$$\eta = -\mathrm{i}\frac{\omega}{g}\phi|_{z=0}. \tag{2}$$

The disturbance coefficient, can thus be defined as:

$$K_d = \eta^P/\eta^I, \tag{3}$$

representing the change in the wave field caused by the presence and action of a body with respect to the

condition with only an incident wave. In a coastal protection perspective, the interest is in minimizing K_d, so as to reduce the impact of the wave field, especially in the lee of the body.

To evaluate the power extraction, the WEC is equipped with a Power Take-Off (PTO) system. These systems often exhibit complex nonlinear behavior (Giorgi & Faedo 2022), largely due to the use of advanced control strategies to maximize power output (Faedo et al. 2022). However, in frequency domain analysis, it is generally possible to linearize the PTO system (Bonfanti & Giorgi 2022), enabling simplification into a spring-damper setup, which facilitates the application of the superposition principle. The equation of motion (Newman 1977) that represents the displacement $\zeta(\omega)$, incorporating the PTO model through the damping matrix, B_{PTO}, and the stiffness matrix, C_{PTO}, is:

$$[-\omega^2(\mathrm{M}+\mathrm{A})+\mathrm{i}\omega(\mathrm{B}+\mathrm{B}_{PTO})+(\mathrm{C}+\mathrm{C}_{PTO})]\zeta=\mathrm{F}. \tag{4}$$

In this equation, M is the body mass matrix, A is the added mass matrix, B is the radiation damping matrix, C represents the hydrostatic and gravitational restoring coefficients, and F denotes the external excitation forces, derived from the sum of diffraction and Froude-Krylov forces (Giorgi et al. 2021).

The boundary value problem is solved using the BEM solver Capytaine (Ancellin & Dias 2019), which is the Python-based implementation of NEMOH, developed at École Centrale de Nantes in France (Babarit & Delhommeau 2015). The simulation domain measures $800\,\mathrm{m} \times 800\,\mathrm{m}$, with a uniform spatial discretization of $2\,\mathrm{m}$ in both the x and y directions. The setup involves positioning either a single WEC or the WEC farm at the center of the domain, keeping the shoreline at a maximum distance of $400\,\mathrm{m}$. This setup is consistent with the requirements for coastal protection and aligns with the shallow water depth required by the chosen WEC technology.
The mean power absorbed by a WEC over a monochromatic wave period is

$$P=\frac{1}{2}\omega^2\zeta^T\mathrm{B}_{PTO}\zeta^*, \tag{5}$$

using the superscripts ^{T} to represent the transpose, and * the complex conjugate.

In this study, different settings of the linear PTO are simulated to analyze the interplay between power production and wave attenuation. In particular, two approaches are defined, the reactive control (indicated by the superscript r) and the passive control (superscript p). The power output is maximized when the damping and stiffness matrices, for a single WEC, have the following configuration, respectively:

$$\begin{cases} B^r_{PTO}=B \\ C^r_{PTO}=(M+A)\,\omega^2-C, \end{cases} \tag{6}$$

$$\begin{cases} B^p_{PTO}=\sqrt{B^2+\frac{1}{\omega^2}\left(-(M+A)\,\omega^2+C\right)^2} \\ C^p_{PTO}=0. \end{cases} \tag{7}$$

It should be noted that these optimal conditions for power extraction apply to a linear, unconstrained, monochromatic system, and might not be as effective in other scenarios. To further evaluate how different control strategies impact WEC performance, the values of B_{PTO} and C_{PTO} are also varied to fine-tune the system's response and allow a wider range of combinations.

3 TEST SETTING

3.1 *Device*

The OSWC is the device chosen for this study, a pitching flap, hinged at its base on a fixed axis anchored to the seabed. It is designed to operate primarily in shallow to intermediate water depths (Hals et al. 2011). The flap's oscillatory motion drives two hydraulic cylinders that connect to the flap and a stationary subframe, producing electricity through an onshore generator. The OSWC is a directional device, performing best when waves have minor spreading.
The flap has a width of $26\,\mathrm{m}$, a thickness of $2\,\mathrm{m}$, and a height of $12\,\mathrm{m}$. Its mass is about $150\,\mathrm{t}$, with a resonance period of approximately $17\,\mathrm{s}$ (corresponding to $0.36\,\mathrm{rad/s}$). In this study, the flap is simplified to have a single degree of freedom ($N_{DOF}=1$), specifically the pitch. It should be noted that the chosen device significantly influences the proposed analysis. The OSWC is selected because it is well suited for coastal protection, being deployed in shallow waters close to the shore, and it generates a larger wake compared to other devices like floating WECs (Battisti et al. 2024). A detailed comparison of the performance of different WECs is beyond the scope of this paper.

3.2 *Case Study*

The farm tested in this study consists of 5 OSWCs, arranged in either a linear or staggered configuration, with a fixed distance between them equivalent to twice the width of the flaps, in both directions. Such distance is based on the minimum requirement for maintenance operations at sea, as commonly referenced in the literature. This distance ensures significant interactions among the WECs, whereas larger distances would result in smaller interactions. Including distance as a variable would introduce additional

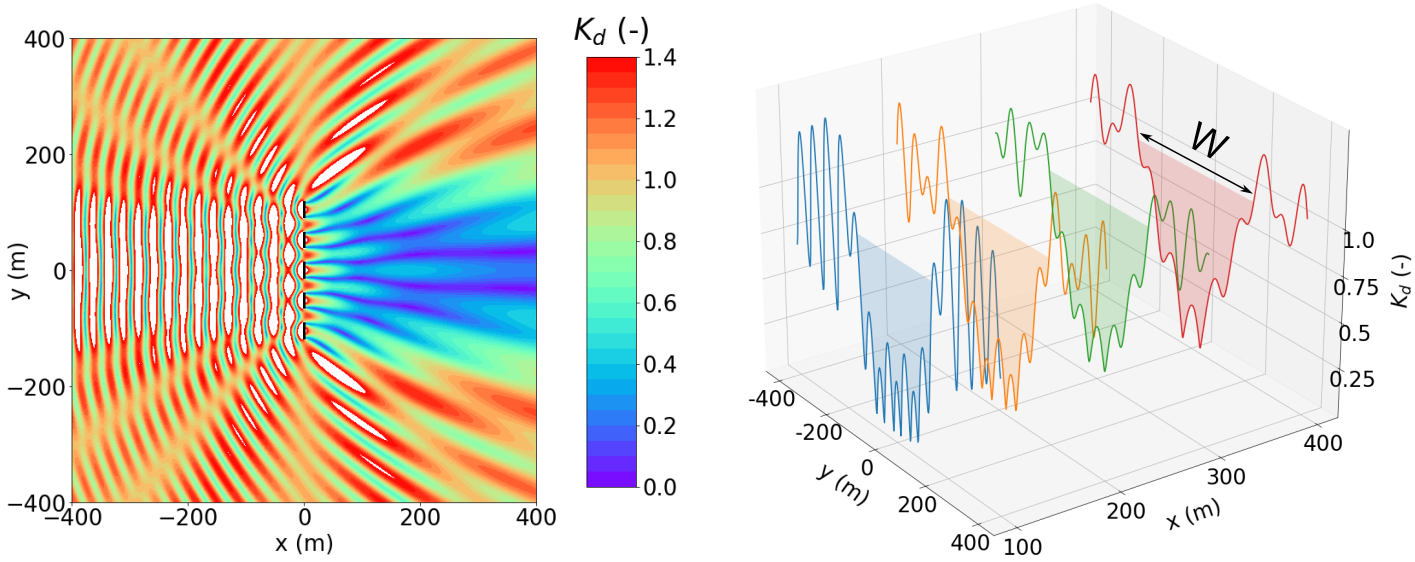

Figure 1: Left: spatial evolution of the K_d coefficient, for $T = 6\,\mathrm{s}$, for a 5-WEC farm in aligned layout. Right: definition of the wake area at different distances in the lee of the farm.

complexity beyond the scope of this paper, but it is an interesting direction for future research. The results presented here cover the range of wave periods, T, from $3\,\mathrm{s}$ to $20\,\mathrm{s}$. The wave period is treated as a parameter, and completes the optimization process afterward, to explore the potential seas aligned with the outcomes.

The main aim of this study is to address a multi-query analysis focused on maximizing both power production and wave attenuation. The first goal is straightforward, but the second requires more careful consideration, and can be challenging to define. A possible approach to wave attenuation is to aim for the maximum possible reduction, but this can be difficult to implement without specific guidelines. Alternatively, a minimum level of wave attenuation can be set, as in this study, which uses a 10% benchmark. This allows the wake width to be calculated to ensure that the wave reduction respects at least the requirement, offering insights into how much of the shoreline could be protected. This study follows this second approach.

As the representation of the K_d coefficient in figure 1 shows, a distinct wake is visible in the lee of the WEC farm. Therefore, to quantify such a wake, a parameter is defined, the wake width W, as the length of the continuous zone where all points have a value of $K_d \leq 0.9$, which represents the 10% wave attenuation. The figure includes various sections taken at different distances from the farm. Since the wake width tends to increase with distance, the results are presented only for $X = 400\,\mathrm{m}$, with other sections showing similar patterns, but smaller values for W.

3.3 *Optimization Strategies*

Various optimization techniques can be pursued depending on the goal. This paper explores the potential to balance two crucial objectives: power generation and wave attenuation, which may potentially be in conflict. While numerous optimization approaches exist, this study considers the following.

- A straightforward strategy is to maximize both wave attenuation and power production, treating them as separate goals. However, this approach might not yield a shared optimum for both objectives, as each is optimized independently.
- By setting a specific requirement, such as a 10% wave attenuation, at a distance of $400\,\mathrm{m}$ from the WEC or WEC farm, it is possible to calculate the maximum power that can be generated under this condition. This approach helps identifying if there are specific frequency ranges or PTO parameters that meet the attenuation target, while also achieving some level of power generation.
- If both objectives need to be optimized simultaneously, a Pareto front approach might be the best solution. The objectives in this case are to maximize the wake width (W), where wave attenuation is at least 10%, while also maximizing the power output (P). This approach allows for exploring the trade-offs between these competing objectives.

4 RESULTS

The initial approach involves maximizing both objectives separately. The test is conducted for both passive and reactive PTO configurations, and with varying PTO parameters.

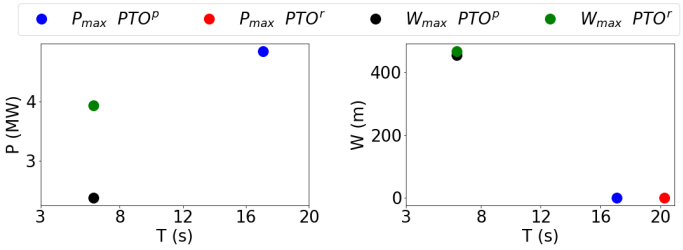

Figure 2: Values of maximum power and maximum wake width for the aligned 5-WEC farm, for the passive and reactive PTO, and with a separate maximization strategy.

Figure 2 illustrates that when the goal is to maximize power output, optimal values are concentrated around large periods, but no wake is generated. In contrast, maximizing the wake width is typically associated with smaller periods and results in less power production. This indicates that the two objectives require very different configurations, often pointing in opposite directions. Specifically, when power output is maximized, the WECs are more active, leading to a more agitated wave field, which contradicts the goal of wave attenuation. On the other hand, a significant wake tends to occur when the WECs are relatively inactive, essentially acting as barriers. It is worth mentioning that the maximum power value for reactive PTO is not shown on the left side of figure 2. Indeed, the system is considered unconstrained as there are no limitations on the flap displacement or the PTO force, which could lead to a nonphysical behavior of the flap. In this case, as the value is not realistic due to the linear assumptions used in the model (for an aligned layout), it is discarded. However, it would occur at a period around 20 seconds, corresponding to the red point on the right side of the figure.

Based on the results in figure 2, three specific periods are selected to examine how power output and wake width evolve with varying PTO parameters. By allowing flexibility in PTO damping and stiffness, greater freedom is introduced into the WEC control strategy. The three chosen periods represent the most common occurrences in the Mediterranean Sea and the ocean. Larger periods, which might offer higher power output, are less likely to generate a wake, in addition to rarely occur, hence they are not the focus of this study.

Figure 3 demonstrates that optimizing power output and wake width individually leads to distinct PTO configurations. The black stars in the graph indicate the optimal points for each objective. For instance, the combination of B_{PTO} and C_{PTO} that maximizes the wake width at $T = 5\,\mathrm{s}$ (bottom left plot) results in minimal or even no power production (top left plot). As the periods increase, particularly from $T = 12\,\mathrm{s}$ onwards, the wake effect diminishes, and vanishes.

The second approach involves ensuring the presence of a wake that achieves 10% wave attenuation, and then defining a suitable range for other parameters, such as period and PTO characteristics, to determine the corresponding power output. This method is adaptable and can be customized for various levels of wave attenuation, depending on the specific site requirements.

Figure 4 illustrates the wake width values as the period and power output are varied. Each point on the graph represents a different combination of PTO parameters. Clearly, not all periods produce a wake, and high power production generally does not generate a wake. When multiple WECs are used, the range of periods that create a wake increases compared to a single WEC (orange points). By adjusting B_{PTO} and C_{PTO}, there are more opportunities to create a wake and generate power, yet the effective period range remains limited to small periods ($T \leq 10\,\mathrm{s}$). This approach aims to achieve wave attenuation first, and then tries to produce energy. While this method addresses both objectives, it may not be optimal for maximizing both wave attenuation and power generation simultaneously.

A multi-objective optimization is therefore needed, which will result in a Pareto front, allowing for the identification of a balanced trade-off between the two goals. In this test, the period is fixed at $T = 5\,\mathrm{s}$, and a variable PTO system is used, where the PTO parameters, B_{PTO} and C_{PTO}, are varied uniformly within a fixed range. Passive and reactive PTO configurations tend to produce predictable results.

Figure 5 shows the possible values of wake width and power for a varying PTO damping coefficient, B_{PTO}. The gray dots represent all available data points, given by each analyzed combination as B_{PTO} is progressively varied in its range. The colored dots are related to the Pareto front for the different values of B_{PTO}. Multiple data points can correspond to each value of B_{PTO}. This figure suggests that higher values of B_{PTO} lead to increased power output and substantial wake width. The largest wake, however, is associated with low B_{PTO} values, where the power output is reduced or even zero.

In figure 6, the stiffness coefficient C_{PTO} is varied, keeping the same period. The resulting trend differs somewhat from the one observed with varying B_{PTO}. Smaller absolute values of C_{PTO} tend to yield higher power output with moderate wake widths. On the other hand, high positive values of C_{PTO} lead to maximum wake widths, though with varying power outputs. High negative values of C_{PTO} generally produce mediocre results. Given these trends, it might be advisable to consider high positive values of C_{PTO}.

5 CONCLUSIONS

Given the relatively low power output of a single WEC with respect to other renewable energy sources, and the need to reduce costs, deploying WEC farms is necessary, and offers additional benefits like coastal protection, which can justify the investment. However, to accurately assess the potential of a WEC farm in terms of both power generation and coastal

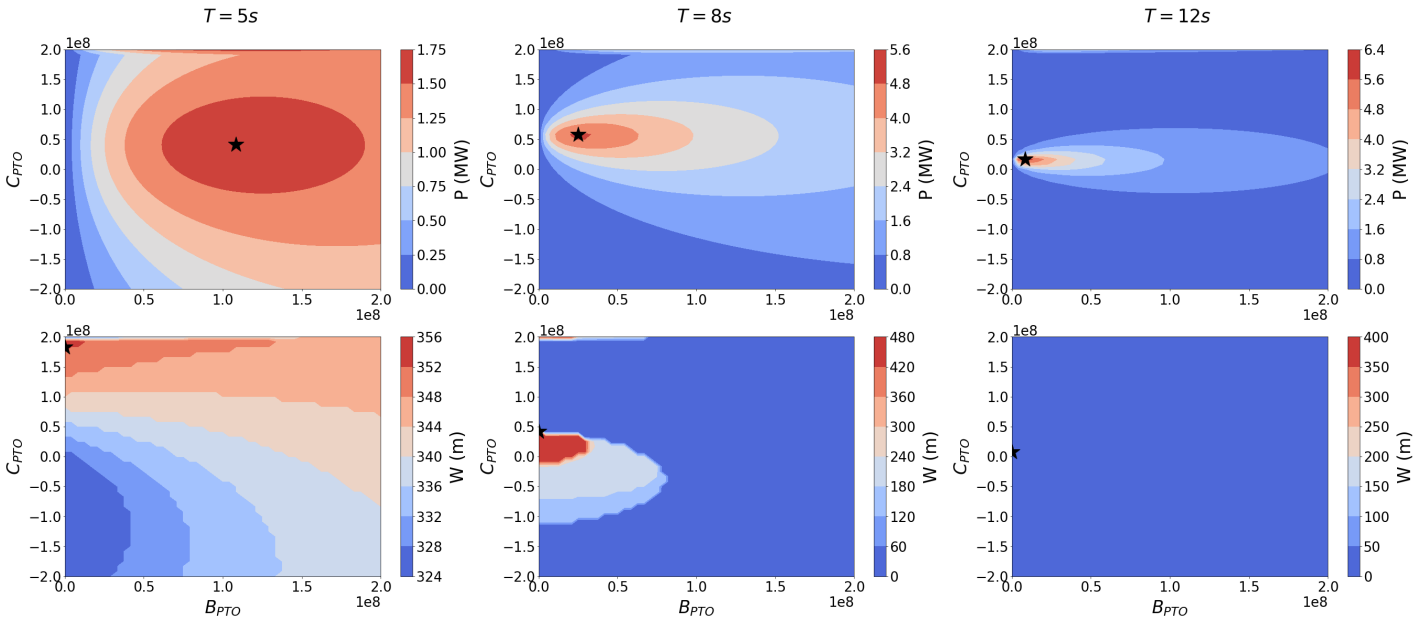

Figure 3: Values of the power output and the wake width at $X = 400\,\mathrm{m}$ for the aligned 5-WEC farm, with varying B_{PTO} and C_{PTO}. Three different periods are represented, $T = 5\,\mathrm{s}$, $T = 8\,\mathrm{s}$, and $T = 12\,\mathrm{s}$. The black stars represent the maximum value of the power and the wake width in the respective representations.

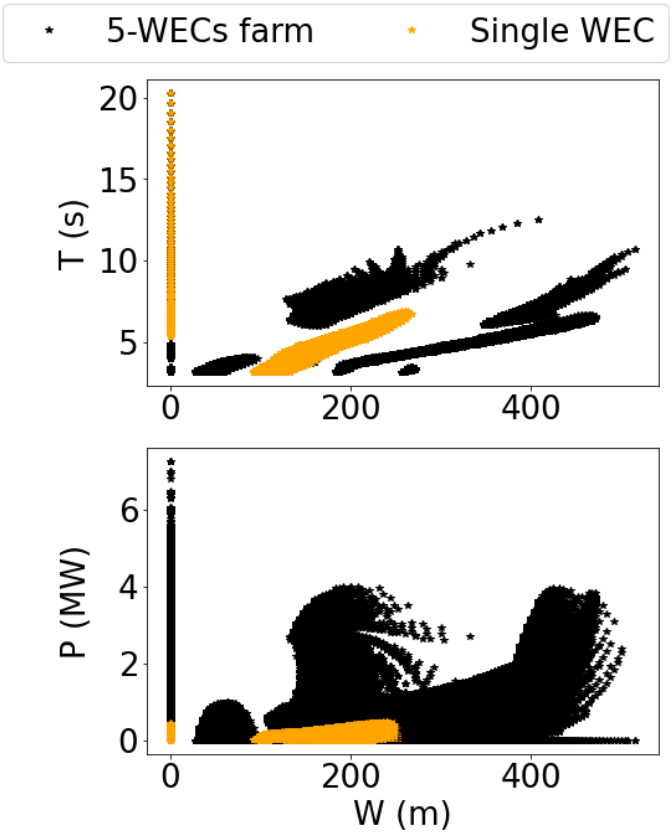

Figure 4: Variation of the wake width with the period (upper part) and the power (lower part) for the 5-WECs aligned farm, compared to a single device case.

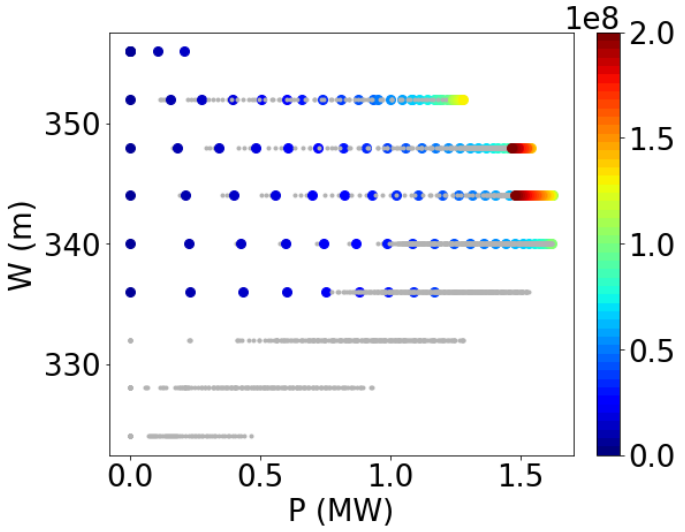

Figure 5: Pareto front for the aligned WEC farm, with varying values of B_{PTO}.

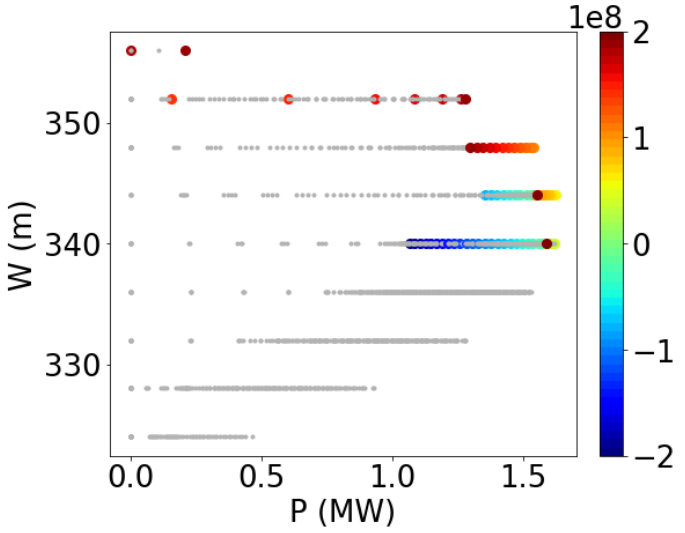

Figure 6: Pareto front for the aligned WEC farm, with varying values of C_{PTO}.

protection, a multi-query analysis is necessary. This study explores the performance of a farm consisting of five OWSCs, in both aligned and staggered configurations. Various approaches are examined to identify potential synergies between the two conflicting objectives of maximizing power production, and maximizing wave attenuation. The results indicate that achieving high power output and substantial wave attenuation require opposite configurations, both in terms of the PTO system and the wave period. The range of periods where a wake is observed is generally limited to small periods, which are, nevertheless, common in both closed and open waters. The best trade-off is determined by seeking a Pareto front, revealing that for a given period, few combinations of PTO damping and stiffness can produce moderate wave attenuation and moderate power output. This research lays the groundwork for future multi-query optimization analyses and supports the feasibility of a dual-purpose WEC farm. Further research includes the investigation of the performance of the WEC farm under panchromatic waves, of different WEC farm layouts, and of different WEC types.

ACKNOWLEDGEMENTS

Project funded under the National Recovery and Resilience Plan (NRRP), Italy, Mission 4 Component 2 Investment 1.3 - Call for tender No. 1561 of 11.10.2022 of Ministero dell' Universitá e della Ricerca (MUR); funded by the European Union – NextGenerationEU Award Number: Project code PE0000021, Concession Decree No. 1561 of 11.10.2022 adopted by Ministero dell'Universitá e della Ricerca (MUR), Italy, CUP, Italy E13C22001890001, Project title "Network 4 Energy Sustainable Transition – NEST". This project has received funding from the European Union's Horizon 2020 research and innovation programme under the Marie Skłodowska-Curie grant agreement No: 101068736.

REFERENCES

Abdulkadir, H., A. Ellithy, & O. Abdelkhalik (2023, 09). Heterogeneous wec array optimization using the hidden genes genetic algorithm. *Proceedings of the European Wave and Tidal Energy Conference 15*.

Ancellin, M. & F. Dias (2019, apr). Capytaine: a Python-based linear potential flow solver. *Journal of Open Source Software 4*(36), 1341.

Babarit, A. & G. Delhommeau (2015). Theoretical and numerical aspects of the open source BEM solver NEMOH. In *Proceedings of the 11th European Wave and Tidal Energy Conference (EWTEC2015)*, Nantes, France.

Battisti, B., G. Giorgi, & G. V. Fernandez (2024). Balancing power production and coastal protection: A bi-objective analysis of wave energy converters. *Renewable Energy 220*, 119702.

Bonfanti, M. & G. Giorgi (2022, oct). Improving Computational Efficiency in WEC Design: Spectral-Domain Modelling in Techno-Economic Optimization. *Journal of Marine Science and Engineering 2022, Vol. 10, Page 1468 10*(10), 1468.

Faedo, N., G. Giorgi, J. V. Ringwood, & G. Mattiazzo (2022). Optimal control of wave energy systems considering nonlinear Froude–Krylov effects: control-oriented modelling and moment-based control. *Nonlinear Dynamics 109*(3), 1777–1804.

Faedo, N., Y. Peña-Sanchez, E. Pasta, G. Papini, F. D. Mosquera, & F. Ferri (2023, aug). SWELL: An open-access experimental dataset for arrays of wave energy conversion systems. *Renewable Energy 212*, 699–716.

Foteinis, S. (2022, jul). Wave energy converters in low energy seas: Current state and opportunities. *Renewable and Sustainable Energy Reviews 162*, 112448.

Foteinis, S. & T. Tsoutsos (2016). Strategies to improve sustainability and offset the initial high capital expenditure of wave energy converters (WECs).

Giglio, E., E. Petracca, B. Paduano, C. Moscoloni, G. Giorgi, & S. A. Sirigu (2023, apr). Estimating the Cost of Wave Energy Converters at an Early Design Stage: A Bottom-Up Approach. *Sustainability 2023, Vol. 15, Page 6756 15*(8), 6756.

Giorgi, G. & N. Faedo (2022, feb). Performance enhancement of a vibration energy harvester via harmonic time-varying damping: A pseudospectral-based approach. *Mechanical Systems and Signal Processing 165*, 108331.

Giorgi, G., S. Sirigu, M. Bonfanti, G. Bracco, & G. Mattiazzo (2021, nov). Fast nonlinear Froude–Krylov force calculation for prismatic floating platforms: a wave energy conversion application case. *Journal of Ocean Engineering and Marine Energy 7*(4), 439–457.

Göteman, M., M. Giassi, J. Engström, & J. Isberg (2020, mar). Advances and Challenges in Wave Energy Park Optimization—A Review.

Hals, J., A. Babarit, A. Kurniawan, & T. Moan (2011). The NumWEC project. Numerical estimation of energy delivery from a selection of wave energy converters – final report. (APRIL).

Kardakaris, K., I. Boufidi, & T. Soukissian (2021, oct). Offshore Wind and Wave Energy Complementarity in the Greek Seas Based on ERA5 Data. *Atmosphere 2021, Vol. 12, Page 1360 12*(10), 1360.

Kazimierczuk, K., C. Henderson, K. Duffy, S. Hanif, S. Bhattacharya, S. Biswas, E. Jacroux, D. Preziuso, D. Wu, D. Bhatnagar, & B. Tarekegne (2023, jun). A socio-technical assessment of marine renewable energy potential in coastal communities. *Energy Research & Social Science 100*, 103098.

Khojasteh, D., A. Shamsipour, L. Huang, S. Tavakoli, M. Haghani, F. Flocard, M. Farzadkhoo, G. Iglesias, M. Hemer, M. Lewis, S. Neill, M. M. Bernitsas, & W. Glamore (2023, aug). A large-scale review of wave and tidal energy research over the last 20 years. *Ocean Engineering 282*, 114995.

Newman, J. N. (1977). *Marine hydrodynamics*. MIT Press Cambridge.

Novo, R., P. Marocco, G. Giorgi, A. Lanzini, M. Santarelli, & G. Mattiazzo (2022). Planning the decarbonisation of energy systems: The importance of applying time series clustering to long-term models. *Energy Conversion and Management: X 15*(January), 100274.

Penalba, M., I. Touzón, J. Lopez-Mendia, & V. Nava (2017). A numerical study on the hydrodynamic impact of device slenderness and array size in wave energy farms in realistic wave climates. *Ocean Engineering 142*, 224–232.

Ringwood, J. V., S. Zhan, & N. Faedo (2023, jan). Empowering wave energy with control technology: Possibilities and pitfalls. *Annual Reviews in Control 55*, 18–44.

Tănase Zanopol, A., F. Onea, & E. Rusu (2014, aug). Coastal impact assessment of a generic wave farm operating in the Romanian nearshore. *Energy 72*, 652–670.

6 APPENDIX

The staggered farm layout yields results comparable to those of the aligned layout, but with generally smaller wake widths due to increased interactions among the devices. The overall trends for maximizing power output and wake width are similar, regardless of the layout, though the differences can be leveraged depending on the desired application. Depending on the priority—either maximizing power production or enhancing wave attenuation—one can adjust the setup accordingly. In this Appendix, the results shown in the paper, for the aligned configuration, are presented for the staggered layout.

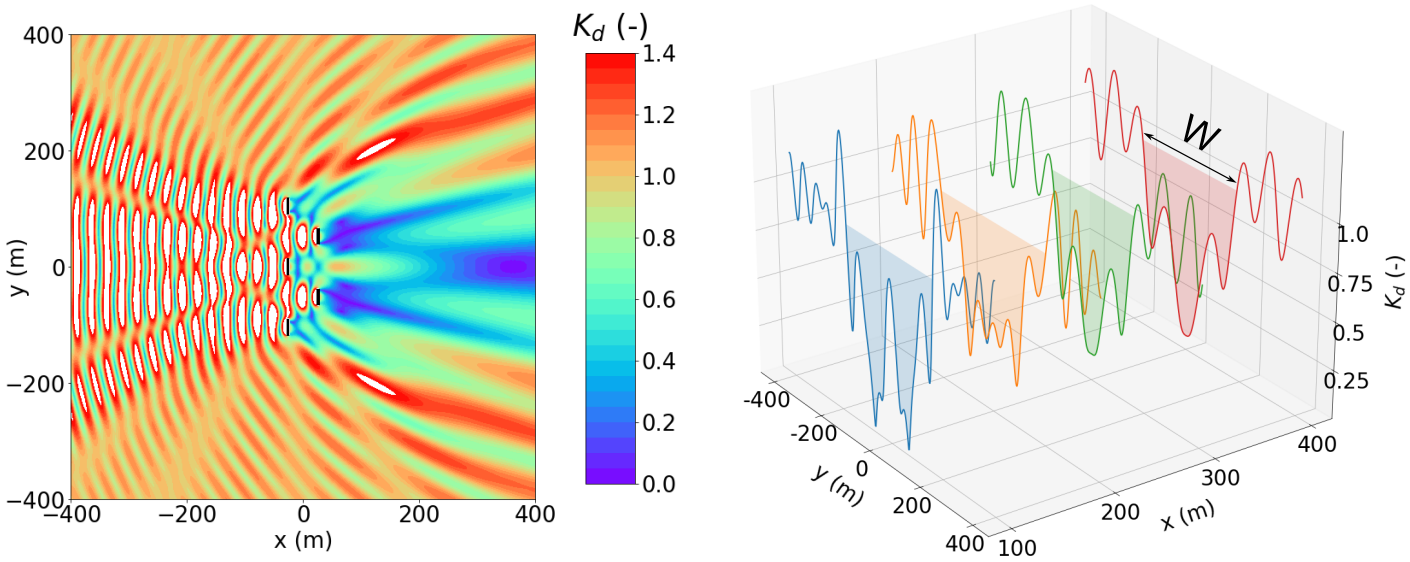

Figure 7: Left: spatial evolution of the K_d coefficient, for $T = 6$ s, for a 5-WEC farm in staggered layout. Right: definition of the wake area at different distances in the lee of the farm.

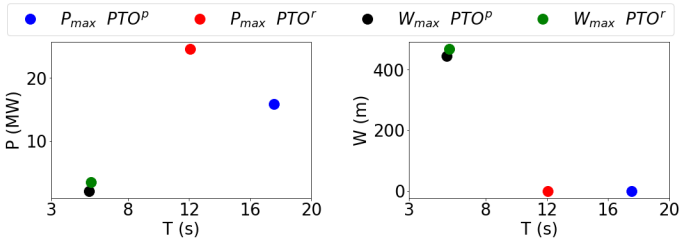

Figure 8: Values of maximum power and maximum wake width for the staggered 5-WEC farm, for the passive and reactive PTO, and with a separate maximization strategy.

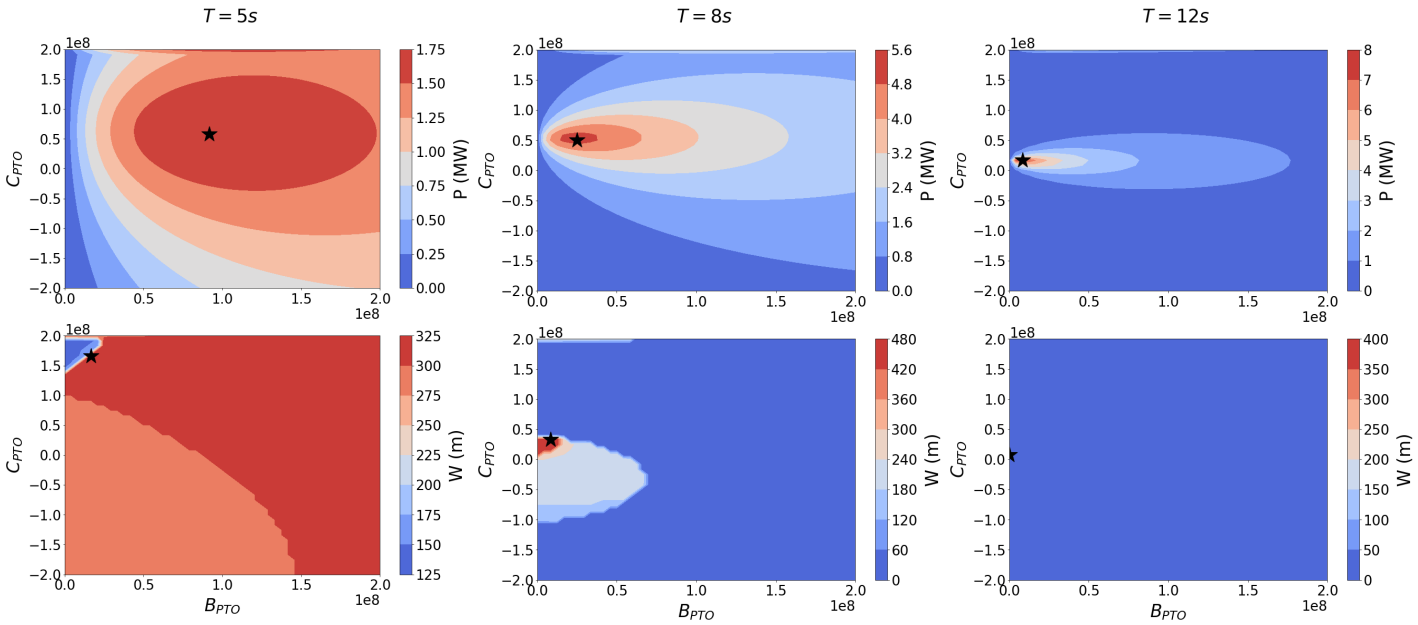

Figure 9: Values of the power output and the wake width at $X = 400\,\text{m}$ for the staggered 5-WEC farm, with varying B_{PTO} and C_{PTO}. Three different periods are represented, $T = 5\,\text{s}$, $T = 8\,\text{s}$, and $T = 12\,\text{s}$. The black stars represent the maximum value of the power and the wake width in the respective representations.

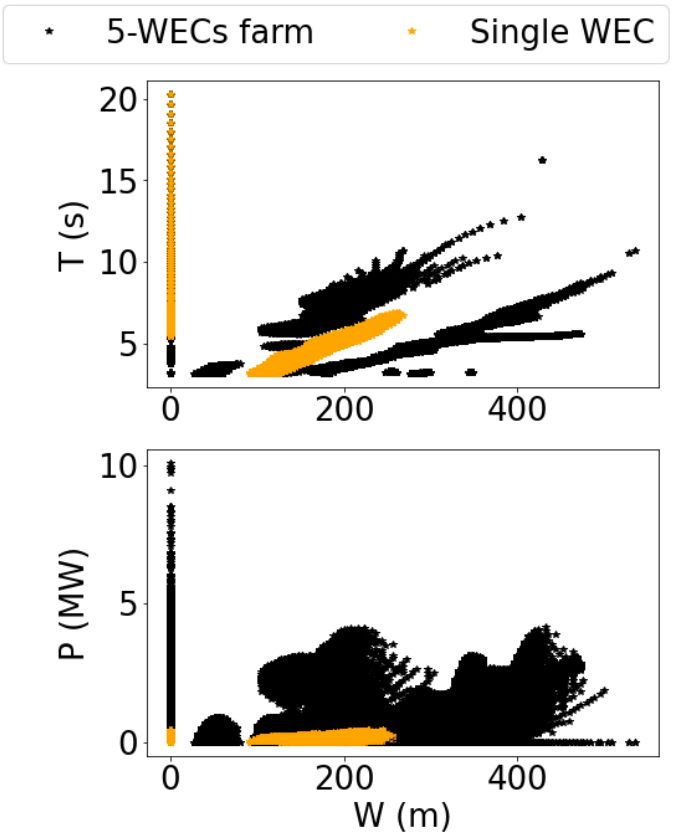

Figure 10: Variation of the wake width with the period (upper part) and the power (lower part) for the 5-WECs staggered farm, compared to a single device case.

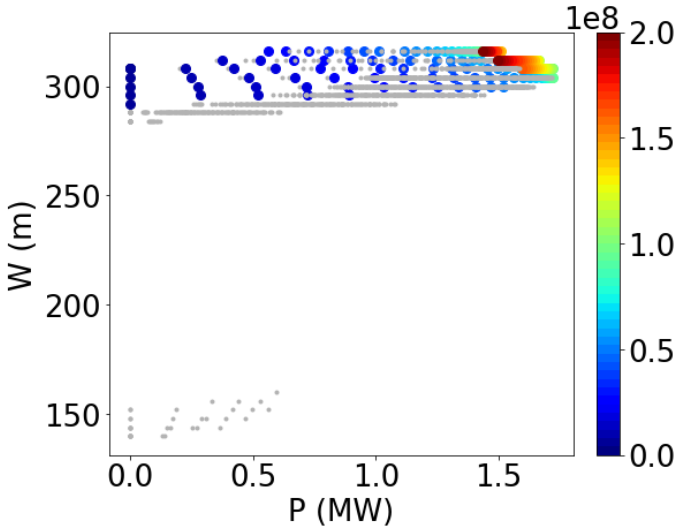

Figure 11: Pareto front for the staggered WEC farm, with varying values of B_{PTO}.

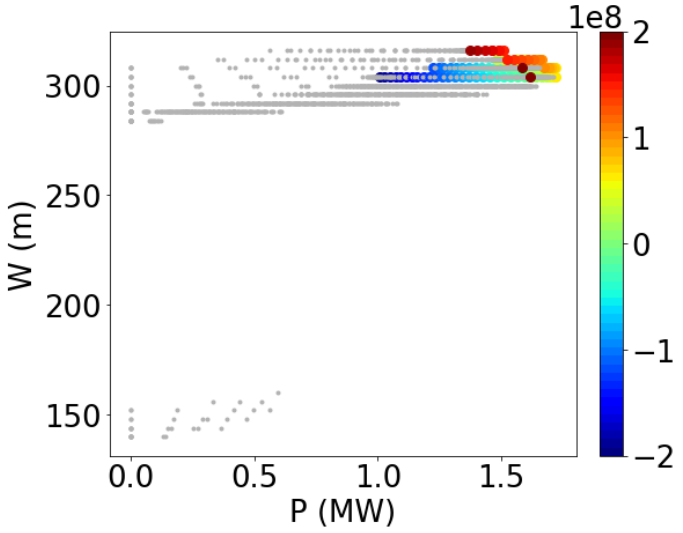

Figure 12: Pareto front for the staggered WEC farm, with varying values of B_{PTO}.